Directed Metalation-Cross Coupling Route to Ferroelectric Liquid Crystals with a Chiral Fluorenol Core: The Effect of Intermolecular Hydrogen Bonding on Polar Order

J. Adam McCubbin,[†] Xia Tong,[‡] Yue Zhao,[‡] Victor Snieckus,*[,†] and Robert P. Lemieux*[,†]

Department of Chemistry, Queen's University, Kingston, Ontario, Canada K7L 3N6, and Département de Chimie, Université de Sherbrooke, Sherbrooke, Québec, Canada J1K 2R1

Received December 8, 2004. Revised Manuscript Received February 28, 2005

The chiral fluorenol mesogen (*R*)-2-(1-octyloxy)-7-((4-undecyloxybenzoyl)oxy)fluoren-9-ol ((*R*)-**3**) was synthesized using a combined directed metalation-cross coupling strategy. The SmC* liquid crystal phase formed by the fluorenol mesogen is more stable and has a wider temperature range than that formed by the fluorenone presursor, which may be ascribed to intermolecular hydrogen bonding. The spontaneous polarization (P_S) of (*R*)-**3** at 10 K below the SmC*-I phase transition temperature is −10.7 nC/cm^2. Molecular modeling based on the Boulder model suggests that the intrinsic conformational bias favoring one orientation of the fluorenol dipole moment along the polar axis of the SmC* phase is very subtle and implies that self-assembly via hydrogen bonding may play a role in enhancing polar order. Results from FT-IR spectroscopy, dilution with achiral SmC additives, and deuterium exchange experiments suggest that the spontaneous polarization is enhanced by the formation of fluorenol dimers via OH−O═C hydrogen bonding. Such self-assembly should increase the rotational order about the long molecular axis and, therefore, the orientational bias of the fluorenol transverse dipole moment along the polar axis that gives rise to P_S.

Introduction

A broad range of liquid crystal phases, including smectic, columnar, and cubic phases, are characterized by varying degrees of positional order which arises from attractive intermolecular interactions and/or amphiphilicity. The self-assembly of amphiphilic molecules in such mesophases usually results from the microsegregation of incompatible structural units such as aromatic versus aliphatic, hydrophilic versus hydrophobic, polar versus nonpolar, fluorinated versus nonfluorinated hydrocarbon, or oligosiloxane versus hydrocarbon chains.[1] Mesomorphic self-assembly can also be achieved via attractive intermolecular interactions such as hydrogen bonding.[2] The first systematic studies of the effect of intermolecular hydrogen bonding on the formation of liquid crystal phases were reported by Gray and Jones more than fifty years ago and focused on the dimerization of 4-alkoxybenzoic acids and *trans*-4-alkoxycinnamic acids.[3] In the ensuing thirty-five years, studies focused primarily on the stabilizing effect of intermolecular hydrogen bonding on mesophases formed by single compounds such as amphiphilic carbohydrates.[4]

In 1989, the first report by Kato and Fréchet of a liquid crystalline heterodimer formed by a pair of complementary hydrogen bond donor and acceptor, 4-butoxybenzoic acid and *trans*-4-(4-ethoxybenzoyloxy)-4′-stilbazole,[5] ushered a period of intense and ongoing activity in the design of supramolecular hydrogen-bonded liquid crystals. In the majority of cases reported thus far, hydrogen bonding promotes the formation of liquid crystal phases via the formation of head-to-head homodimers or complementary heterodimers.[2] Only in a few cases has lateral intermolecular hydrogen bonding been shown to enhance positional order and thus promote the formation of lamellar smectic phases, including the orthogonal smectic A (SmA) and tilted smectic C (SmC) phases.[6]

When a SmC phase is formed by chiral molecules (SmC*), it exhibits a spontaneous polarization (P_S) along a polar C_2 axis perpendicular to the plane defined by the molecular long axis (director) **n** and the layer normal **z**.[7] By coupling the

* Corresponding authors. E-mails: lemieux@chem.queensu.ca, snieckus@chem.queensu.ca.
[†] Queen's University.
[‡] Université de Sherbrooke.

(1) For recent reviews, see: (a) Tschierske, C. *J. Mater. Chem.* **2001**, *11*, 2647. (b) Tschierske, C. *J. Mater. Chem.* **1998**, *8*, 1485.
(2) For recent reviews, see: (a) Kato, T.; Mizoshita, N.; Kanie, K. *Macromol. Rapid Commun.* **2001**, *22*, 797. (b) Paleos, C. M.; Tsiourvas *Liq. Cryst.* **2001**, *28*, 1127. (c) Kato, T. *Struct. Bonding* **2000**, *96*, 95. (d) Kato, T. In *Handbook of Liquid Crystals*; Demus, D., Goodby, J. W., Gray, G. W., Spiess, H.-W., Vill, V., Eds.; Wiley-VCH: Weinheim, Germany, 1998; Vol. 2B, pp 969−978. (e) Prade, H.; Miethchen, R.; Vill, V. *J. Prakt. Chem.* **1995**, *337*, 427.
(3) (a) Gray, G. W.; Jones, B. *J. Chem. Soc.* **1953**, 4179. (b) Gray, G. W.; Jones, B. *J. Chem. Soc.* **1954**, 1467.
(4) Jeffrey, G. *Acc. Chem. Res.* **1986**, *19*, 168.
(5) Kato, T.; Frechet, J. M. J. *J. Am. Chem. Soc.* **1989**, *111*, 8533.
(6) (a) Kajitani, T.; Kohmoto, S.; Yamamoto, M.; Kishikawa, K. *Chem. Mater.* **2004**, *16*, 2329. (b) Plehnert, R.; Schroter, J. A.; Tschierske, C. *J. Mater. Chem.* **1998**, *8*, 2611. (c) Hildebrandt, F.; Schröter, J. A.; Tschierske, C.; Festag, R.; Kleppinger, R.; Wendorff, J. H. *Angew. Chem., Int. Ed. Engl.* **1995**, *34*, 1631. (d) Mori, A.; Takeshita, H.; Nimura, R.; Isobe, M. *Liq. Cryst.* **1993**, *14*, 821. (e) Malthéte, J.; Levelut, A.-M.; Liébert, L. *Adv. Mater.* **1992**, *4*, 37. (f) Matsunaga, Y.; Terada, M. *Mol. Cryst. Liq. Cryst.* **1986**, *141*, 321. (g) Schubert, H.; Hoffmann, S.; Hauschild, J. *Z. Chem.* **1977**, *17*, 414. (h) Lochmüller, C. H.; Souter, R. W. *J. Phys. Chem.* **1973**, *77*, 3016.
(7) Meyer, R. B.; Liebert, L.; Strzelecki, L.; Keller, P. *J. Phys. (Paris) Lett.* **1975**, *36*, L69.

10.1021/cm047860p CCC: $30.25
Published on Web 04/15/2005

spontaneous polarization to an electric field, the ferroelectric SmC* phase can be switched between opposite tilt orientations on a microsecond time scale and function as an electrooptical light shutter between crossed polarizers.[8,9] The spontaneous polarization is a chiral bulk property which originates from a conformational preference of transverse molecular dipoles to orient in one direction along the polar axis due to steric coupling between polar functional groups and the stereogenic center (stereopolar coupling).[10,11] In the few reported cases of ferroelectric SmC* phases formed by hydrogen bonding of complementary molecules,[12] the self-assembly is achieved via head-to-head hydrogen bonding of complementary pairs such as the benzoic acid/stilbazole complex **1** in which the stereogenic center is located in the side-chain, at a position remote from the site of hydrogen bonding. Thus, intermolecular hydrogen bonding promotes the formation of the SmC* phase but does not contribute to the spontaneous polarization because the hydrogen bond is oriented along the molecular long axis **n** and has no conformational asymmetry due to a lack of stereo-polar coupling. In principle, lateral intermolecular hydrogen bonding could promote the formation of a SmC* phase *and* enhance its spontaneous polarization by forming a hydrogen bond network with polar order along the C_2 axis of the SmC* phase, provided that the hydrogen bonding group is coupled to the stereogenic center.[13]

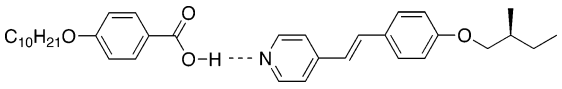

1

Recently, we reported the synthesis and characterization of a series of ferroelectric SmC* liquid crystals with a chiral fluorenol core (e.g., **2**) using a combined directed metalation-Suzuki cross coupling strategy.[14] The SmC* phase formed by the fluorenol mesogens is more stable than that formed by the corresponding fluorenone mesogens, which was ascribed to intermolecular hydrogen bonding based on variable-temperature FT-IR spectroscopy. The difference in spontaneous polarization between the (*R*,*R*) and (*S*,*R*) diastereomers of **2** (+58 and +100 nC/cm^2, respectively) is consistent with polar ordering of the fluorenol core, which may be due in part to steric coupling of the core to the chiral side-chain. However, the extent to which intermolecular hydrogen bonding contributes to polar ordering of the core remained in question. To address this problem, we have synthesized the ferroelectric SmC* mesogen (*R*)-**3** with the fluorenol core as the only chiral element and measured its spontaneous polarization. Results of dilution experiments with achiral SmC mesogens, deuterium exchange, and FT-IR measurements suggest that the formation of hydrogen-bonded dimers in the SmC* phase plays an essential role in amplifying the polar order of the fluorenol core, giving rise to a measurable spontaneous polarization.

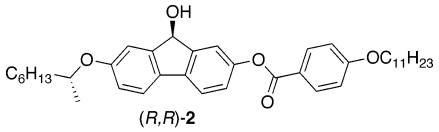

(*R*,*R*)-**2**

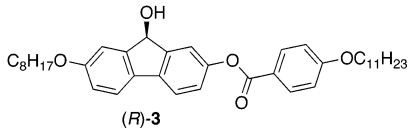

(*R*)-**3**

Results

Synthesis. Compound (*R*)-**3** was synthesized in optically pure form based on a modification of the route first reported for the synthesis of **2** (Scheme 1).[14] Alkylation of the intermediate **4** was followed by conversion of the Br group to OH via lithium−halogen exchange, trapping with B(O-*i*-Pr)$_3$ and oxidation with hydrogen peroxide to give **6** in 80% yield. The OH group was protected as a methoxymethyl ether (82%), and cyclization to the fluorenone **8** was achieved in 67% yield via a directed remote metalation (DreM) reaction using LDA. Deprotection and esterification of **9** using DCC/DMAP gave the achiral fluorenone **11** in 82% yield. Chemoselective reduction of **11** with $NaBH_4$ gave the racemic fluorenol **3** in quantitative yield. We were unable to resolve the enantiomers of **3** by chiral stationary phase HPLC, but were successful in resolving the enantiomers of the fluorenediol **10** in optically pure form (>99% ee) using a semipreparative Daicel Chiralpak-AS column. The (*S*) absolute configuration was assigned to the first eluted enantiomer of **10** based on the reasonable assumption that the elution order should be the same as that observed with the diastereomeric fluorenediol precursors to **2**.[15] The resolved fluorenediol was then esterified selectively using 1-(4-undecyloxybenzoyl)triazole under basic conditions to give the mesogen (*R*)-**3** in 56% yield.

(8) Clark, N. A.; Lagerwall, S. T. *Appl. Phys. Lett.* **1980**, *36*, 899.
(9) (a) Lagerwall, S. T. *Ferroelectric and Antiferroelectric Liquid Crystals*; Wiley-VCH: Weinheim, Germany, 1999. (b) Lagerwall, S. T. In *Handbook of Liquid Crystals*; Demus, D., Goodby, J. W., Gray, G. W., Spiess, H. W., Vill, V., Eds.; Wiley-VCH: Weinheim, Germany, 1998; Vol. 2B. (c) Walba, D. M. *Science* **1995**, *270*, 250. (d) Clark, N. A., and Lagerwall, S. T. In *Ferroelectric Liquid Crystals: Principles, Properties and Applications*; Goodby, J. W., Blinc, R., Clark, N. A.; Lagerwall, S. T.; Osipov, M. A.; Pikin, S. A.; Sakurai, T.; Yoshino, K.; Zeks, B., Eds.; Gordon and Breach: Philadelphia, 1991; pp 409−452. (e) Dijon, J. In *Liquid Crystals: Applications and Uses*; Bahadur, B., Ed.; World Scientific: Singapore, 1990; Vol. 1, Chapter 13.
(10) Goodby, J. W. In *Ferroelectric Liquid Crystals: Principles, Properties and Applications*; Goodby, J. W., Blinc, R., Clark, N. A., Lagerwall, S. T., Osipov, M. A., Pikin, S. A., Sakurai, T., Yoshino, K., Zeks, B., Eds.; Gordon & Breach: Philadelphia, 1991; p 99−157.
(11) Walba, D. M. In *Advances in the Synthesis and Reactivity of Solids*; Mallouck, T. E., Ed.; JAI Press: Greenwich, CT, 1991; Vol. 1, p 173.
(12) (a) Sridevi, B.; Chalapathi, P. V.; Srinivasulu, M.; Pisipati, V. G. K. M.; Potukuchi, D. M. *Liq. Cryst.* **2004**, *31*, 303. (b) Tian, Y.; Xu, X.; Zhao, Y.; Tang, X.; Li, T. *Liq. Cryst.* **1997**, *22*, 87. (c) Kihara, H.; Kato, T.; Uryu, T.; Ujiie, S.; Kumar, U.; Fréchet, J. M. J.; Bruce, D. W.; Price, D. J. *Liq. Cryst.* **1996**, *21*, 25. (d) Tian, Y.; Su, F.; Zhao, Y.; Luo, X.; Tang, X.; Zhao, X.; Zhou, E. *Liq. Cryst.* **1995**, *19*, 743. (e) Yu, L. J. *Liq. Cryst.* **1993**, *14*, 1303. (f) Kato, T.; Kihara, H.; Uryu, T.; Ujiie, S.; Iimura, K.; Fréchet, J. M. J.; Kumar, U. *Ferroelectrics* **1993**, *148*, 161. (g) Kumar, U.; Fréchet, J. M. J.; Kato, T.; Ujiie, S.; Timura, K. *Angew. Chem., Int. Ed. Engl.* **1992**, *31*, 1531.
(13) An example of polar order in a nonlinear optical thin film promoted by intermolecular hydrogen bonding was recently reported: Rashid, A. N.; Erny, C.; Gunter, P. *Adv. Mater.* **2003**, *15*, 2024.
(14) McCubbin, J. A.; Tong, X.; Wang, R.; Zhao, Y.; Snieckus, V.; Lemieux, R. P. *J. Am. Chem. Soc.* **2004**, *126*, 1161.
(15) We have shown that the interaction of the fluorenediol moiety with the amylose carbamate chiral stationary phase of the Chiralpak-AS column is essential for resolution to be achieved.[14]

Scheme 1[a]

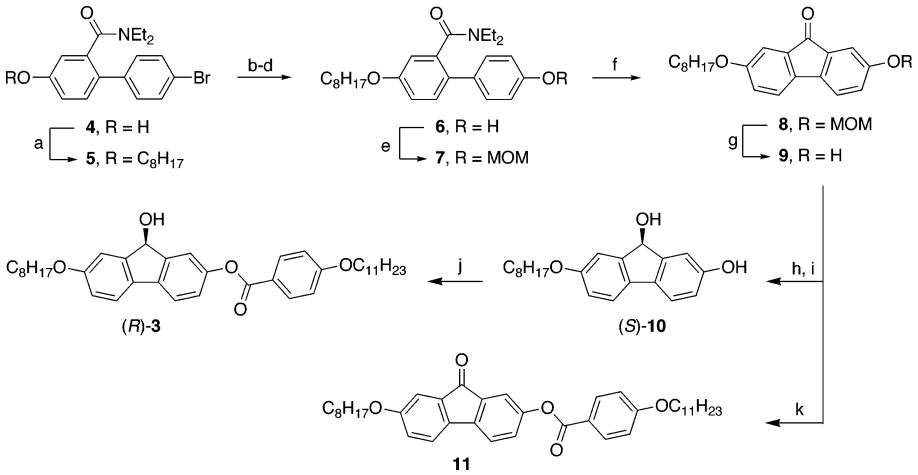

[a] Reagents and conditions: (a) *n*-$C_8H_{17}Br$, K_2CO_3, MeCN, reflux, 96%; (b) 2.6 M *n*-BuLi, THF, −78 °C; (c) $B(O\text{-}iPr)_3$, −78 to 25 °C; (d) 35% aq H_2O_2, 0 °C, 83%; (e) (MOM)Cl, CH_2Cl_2, *i*-Pr_2NEt, 25 °C, 82%; (f) 1.0 M LDA, THF, 0 to 25 °C, 67%; (g) 6 M aq HCl, *i*-PrOH, 25 °C, 96%; (h) $NaBH_4$, 1:1 MeOH/Et_2O, 25 °C, 99%; (i) semiprep HPLC resolution, Daicel Chiralpak-AS column, 20% *i*-PrOH/hexanes, 3.0 mL/min; (j) 1-(4-undecyloxybenzoyl)-benzotriazole, 0.5 M aq NaOH, THF, 25 °C, 56%; (k) 4-undecyloxybenzoic acid, DCC, DMAP, CH_2Cl_2, 25 °C, 85%.

Scheme 2[a]

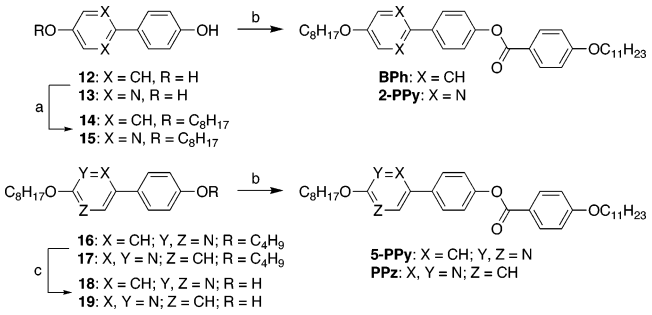

[a] Reagents and conditions: (a) *n*-$C_8H_{17}Br$, K_2CO_3, MeCN, reflux, 45−51%; (b) 4-undecyloxybenzoic acid, DCC, DMAP, CH_2Cl_2, 25 °C, 79−83%; (c) BBr_3, CH_2Cl_2, −78 to 25 °C, 76−77%.

Table 1. Liquid Crystalline Properties

compound	phase sequence[a]
11	Cr 91 (24.8) SmC 129 (2.0) N 152 (2.5) I
(*RS*)-**3**	Cr 86 (22.0) SmC 168 (9.4) I
(*R*)-**3**	Cr 87 SmC* 181 I[b]
BPh	Cr 122 (42.6) SmC 169 (4.2) N 183 (2.4) I
2-PPy	Cr 83 (51.5) SmC 113 (1.6) N 183 (3.0) I
5-PPy	Cr 92 (5.6) SmC 116[b] SmA 190 (10.9) I
PPz	Cr 95 (26.0) SmC 104 (15.0) I

[a] Phase transition temperatures (°C) and enthalpies of transition (kJ/mol) (in parentheses) were measured on heating by DSC at a rate of 5 K/min. [b] Phase transition temperatures measured by polarized microscopy.

To assess the effect of intermolecular hydrogen bonding on polar order in the SmC* phase formed by (*R*)-**3**, a series of achiral SmC mesogens with the same side-chains but different core structures were synthesized (Scheme 2) and used in dilution experiments with (*R*)-**3** (vide infra). Monoalkylation of 4,4′-biphenol (**12**) and4′-hydroxy-2-phenylpyrimidin-5-ol (**13**) with 1 equiv of 1-bromooctane gave the precursors **14** and **15** in 45% and 51% yield, respectively. The regiochemistry of **15** was confirmed by heteroatom multi-bond correlation (HMBC) NMR (see Supporting Information). The corresponding 5-phenylpyrimidine and 6-phenylpyridazine precursors **18** and **19** were obtained in 77% and 76% yield, respectively, by selective BBr_3-mediated cleavage of the 4′-butyloxy groups in mesogens **16** and **17**, which had been prepared in a previous study.[16,17] Esterification of the four precursors using DCC/DMAP gave the mesogens **BPh**, **2-PPy**, **5-PPy**, and **PPz** in 79−83% yield. To further assess the effect of hydrogen bonding on mesophase stability and polar order, the fluorenol **3** was methylated using NaH and MeI. However, the methyl ether did not form a liquid crystal phase, which may be ascribed to an unfavorable increase in lateral bulk combined with weaker intermolecular interactions.[6c]

Mesophase Characterization. The liquid crystal phases formed by the fluorenol **3** as a racemic mixture (*RS*) and homochiral form (*R*), and by the achiral compounds **11**, **BPh**, **2-PPy**, **5-PPy**, and **PPz** were characterized by polarized optical microscopy and differential scanning calorimetry (Table 1). The achiral fluorenone **11** forms enantiotropic nematic and SmC phases, which are characterized by the Schlieren and broken fan textures shown in panels a and b, respectively, of Figure 1. The corresponding fluorenols (*RS*)-**3** and (*R*)-**3** form enantiotropic SmC and SmC* phases that persist to room temperature on cooling. Both the racemic and homochiral forms of **3** produced a gray Schlieren texture as a thin film between glass slide and cover slip (Figure 1c). As previously observed with the diastereomeric fluorenol **2**,[14] (*RS*)-**3** and (*R*)-**3** have broader smectic temperature ranges and higher clearing points than the corresponding fluorenone **11**. This observation, along with the significant difference in clearing point between the racemic (*RS*)-**3** and resolved (*R*)-**3**, suggest that intermolecular hydrogen bonding interactions involving the chiral fluorenol core play an important role in stabilizing the SmC phase.[6] The mesomorphic properties of **BPh**, **2-PPy**, **5-PPy**, and **PPz** are consistent

(16) Hegmann, T.; Meadows, M. R.; Wand, M. D.; Lemieux, R. P. *J. Mater. Chem.* **2004**, *14*, 185.

(17) The regioselectivity of this reaction may be due to the weaker coordination ability of the alkoxy group on the heterocyclic ring. Selective deprotection of anisole over 2-methoxypyridine derivatives has been reported previously: Groziak, M. P. U.S. Patent 6,083,936, 2000; *Chem. Abstr.* **2000**, *133*, 68925.

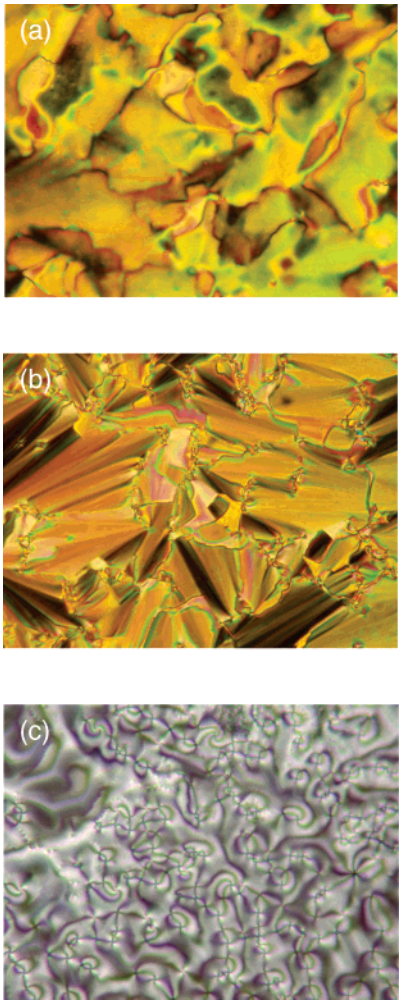

Figure 1. Polarized photomicrographs of (a) **11** in the nematic phase at 135 °C (500×), (b) **11** in the SmC phase at 122 °C (500×), and (*RS*)-**3** in the SmC phase at 140 °C (500×).

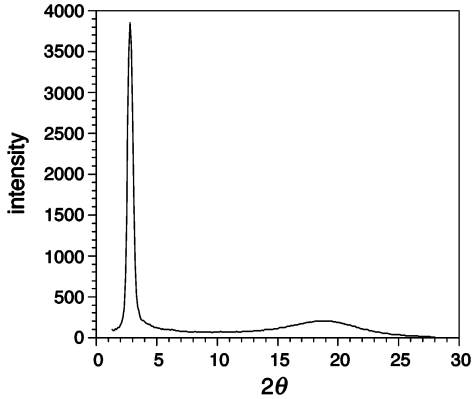

Figure 2. Powder X-ray diffraction intensity profile for (*RS*)-**3** at 160 °C on heating.

with empirical trends for mesogens with similar variations in core structure.[16,18]

Further analysis of (*RS*)-**3** by variable-temperature powder X-ray diffraction confirmed the SmC phase assignment. As shown in Figure 2, a single sharp peak was observed at a constant Bragg angle 2θ of 2.79°, which suggests a temperature invariance of the tilt angle that is characteristic of materials with a first-order SmC−I transition. A broad halo at wider angle is consistent with the diffuse lamellar structure of the SmC phase. The small angle 2θ value corresponds to a smectic layer spacing of 31.8 Å, which is significantly shorter than the calculated molecular length (vide infra) and is consistent with a tilted lamellar structure.

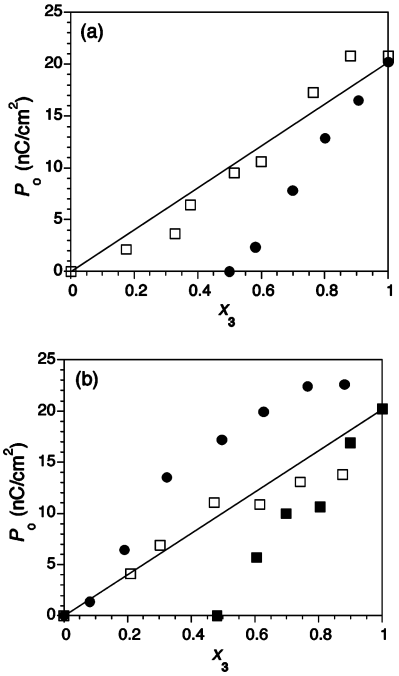

Figure 3. Absolute values of reduced polarization (P_o) as a function of the mole fraction of (*R*)-**3** in mixtures with (a) **11** (filled circles), **BPh** (open squares), and (b) **2-PPy** (filled circles), **5-PPy** (open squares), and **PPz** (filled squares) measured at $T - T_C = -10$ K.

Polarization Measurements. The spontaneous polarization (P_S) and tilt angle θ were measured as a function of temperature for (*R*)-**3** as a surface-stabilized 4 μm film. At 10 K below the SmC*-I transition temperature ($T - T_C = -10$ K), the spontaneous polarization is −10.7 nC/cm^2 and the optical tilt angle is 32°, which corresponds to a reduced polarization (P_o) of −20.2 nC/cm^2.[19] To determine whether this spontaneous polarization originates from an intrinsic conformational bias of the fluorenol dipoles to orient in one direction along the polar axis or from the formation of a polar hydrogen bond network by the fluorenol cores, we carried out a series of experiments in which (*R*)-**3** was incrementally diluted with achiral SmC mesogens with no hydrogen bond donor group (**11**, **BPh**, **2-PPy**, **5-PPy**, **PPz**). The reduced polarizations of the resulting mixtures were measured at $T - T_C = -10$ K and plotted (as absolute values) as a function of the fluorenol mole fraction x_3 (Figure 3). The results show three distinct effects of dilution on P_o depending on the core structure of the additive. Dilution with the fluorenone **11** and the phenylpyridazine **PPz** caused P_o to decrease nonlinearly, reaching a value of ≤0.3 nC/cm^2 (the detection limit of our instrument) at $x_3 = 0.50$, which

(18) Goodby, J. W. In *Handbook of Liquid Crystals*; Demus, D., Goodby, J. W., Gray, G. W., Spiess, H.-W., Vill, V., Eds.; Wiley-VCH: Weinheim, Germany, 1998; Vol. 2A, p 411.

(19) According to phenomenological theory, the spontaneous polarization P_S and tilt angle θ of a SmC* phase are related to the reduced polarization P_o according to the equation $P_o = P_S \sin \theta^{-1}$. The reduced polarization is intrinsic to the chiral component of the SmC* phase at a fixed reduced temperature $T - T_C$. Kuczynski, W.; Stegemeyer, H. *Chem. Phys. Lett.* **1980**, *70*, 123.

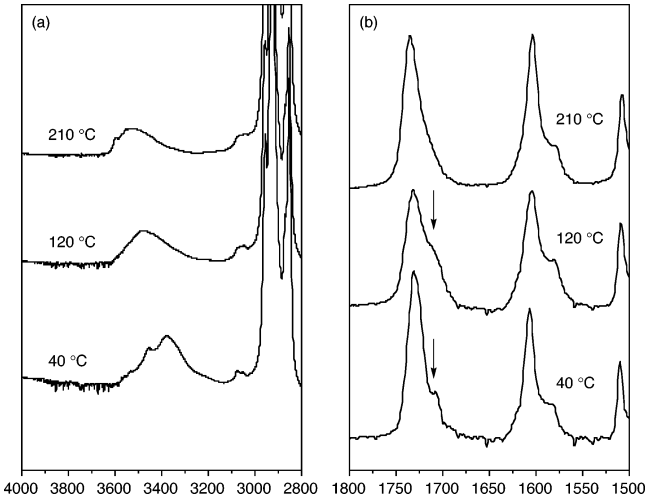

Figure 4. FT-IR spectra of (*R*)-**3** as a thin film taken in the crystalline phase (40 °C), in the SmC* phase (120 °C) and in the isotropic liquid phase (210 °C).

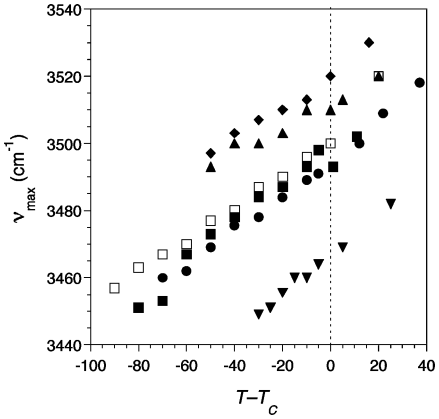

Figure 5. OH stretching frequency ν_{max} as a function of reduced temperature $T - T_C$ for (*R*)-**3** (open squares) and 1:1 mixtures of (*R*)-**3** with **11** (triangles), **BPh** (diamonds), **5-PPy** (filled squares), **2-PPy** (circles), and **PPz** (inverted triangles).

is consistent with the perturbation of a polar network. Interestingly, dilution with the biphenyl **BPh** and 5-phenylpyrimidine **5-PPy** caused P_o to decrease more or less linearly, whereas dilution with the 2-phenylpyrimidine **2-PPy** caused P_o to increase in absolute value between $x_3 = 1.0$ and 0.60, with the P_o versus x_3 plot showing a positive deviation from linearity overall. The latter suggests that intermolecular interactions with **2-PPy** reinforce the polar order of (*R*)-**3**, and is inconsistent with the presence of an extended polar hydrogen bond network in the SmC* phase of (*R*)-**3**.

FT-IR Spectroscopy. To determine the nature and extent of hydrogen bonding in the SmC* phase formed by (*R*)-**3** and by the mixtures of (*R*)-**3** and achiral SmC mesogens, FT-IR spectra of thin films were acquired as a function of temperature.[20] As previously observed with the diastereomeric fluorenol **2**,[14] the IR spectrum of (*R*)-**3** in the crystalline phase (40 °C) features a strong ester C═O stretch band at 1730 cm^{-1} together with a weaker band at 1707 cm^{-1} that is assigned to hydrogen-bonded carbonyl groups (arrow in Figure 4). The latter becomes more prominent upon heating into the SmC* phase (120 °C) and disappears upon further heating into the isotropic liquid phase (210 °C). Two overlapping O−H stretch bands at 3380 and 3450 cm^{-1} can be distinguished in the crystalline phase, which are assigned to hydrogen bonded OH groups (i.e., self-associated) and OH groups hydrogen bonded to carbonyl groups, respectively. The OH stretch band gradually shifts to higher wavenumbers upon heating from the crystalline to the SmC* phase (Figures 4 and 5), which is consistent with a shift in the distribution of hydrogen bonds—from OH−OH interactions to OH−O═C interactions—and a weakening of hydrogen bonding interactions on average.

To determine the extent of hydrogen bonding between (*R*)-**3** and the various SmC additives used in the dilution experiments, the peak OH stretch frequency ν_{max} was measured as a function of the reduced temperature ($T - T_C$) for 1:1 mixtures of (*R*)-**3** and each of the SmC additives. As shown in Figure 5, the addition of **BPh** caused the largest positive shift in ν_{max}, which may be ascribed to the lack of hydrogen bond accepting group in the biphenyl core. Interestingly, the fluorenone **11** caused a comparable positive shift in ν_{max} despite the presence of the carbonyl group in the core. No significant shift was observed with the two phenylpyrimidine additives **2-PPy** and **5-PPy**, which suggests that the formation of OH−N hydrogen bonds compensates for the perturbation of hydrogen bonds. The addition of **PPz** caused a significant negative shift in ν_{max}, which is likely due to the superior hydrogen bond accepting ability of pyridazine relative to hydroxy and carbonyl groups.[21]

Deuterium Isotope Effect. The effect of hydrogen bond perturbations on the polar order of (*R*)-**3** was also investigated by deuterium exchange, a method that is often used to study the role of hydrogen bonding in the stabilization of secondary and tertiary protein structures.[22] Hence, the spontaneous polarization of (*R*)-**3** was measured as a function of temperature before and after deuterium exchange, which was achieved by stirring the fluorenol in a 1:1 mixture of CD_3OD and $CDCl_3$ for 1 h (Figure 6). The experiment was carried out in duplicate under conditions that rigorously excluded protic solvents. In both cases, deuterium exchange resulted in an increase in spontaneous polarization by ca. 35% at $T - T_C = -10$ K.

Molecular Modeling. The intrinsic conformational bias of (*R*)-**3** giving rise to polar order in the SmC* phase was evaluated by molecular modeling (AM1) based on the assumptions of the Boulder model.[11] To simplify the conformational distribution, it is assumed that the plane of the fluorenol core is congruent with the tilt plane of the SmC* phase, with the carbinol C−O dipole moment in one of two possible orientations along the polar axis, and that the alkoxy

(20) For a recent example of the use of variable temperature FT-IR spectroscopy to probe hydrogen bonding interactions in smectic liquid crystals, see: Jang, W. G.; Park, C. S.; Kim, K. H.; Glaser, M. A.; Clark, N. A. *Phys. Rev. E* **2000**, *62*, 5027.

(21) (a) Kim, J. H.; Li, H.-J.; Kim, E.-J.; Jung, H. J.; Young-Sang, C.; Park, J.; Yoon, C.-J. *J. Phys. Chem. A* **2004**, *108*, 921. (b) Kasende, O.; Zeegers-Huyskens, T. *J. Phys. Chem.* **1984**, *88*, 2132.

(22) For recent examples, see: (a) Eker, F.; Griebenow, K.; Schweitzer-Stenner, R. *J. Am. Chem. Soc.* **2003**, *125*, 8178. (b) Krantz, B. A.; Srivastava, A. K.; Nauli, S.; Baker, D.; Sauer, R. T.; Sosnick, T. R. *Nature Struct. Biol.* **2002**, *9*, 458. (c) Shi, Z.; Krantz, B. A.; Kallenbach, N.; Sosnick, T. R. *Biochemistry* **2002**, *41*, 2120, and references therein.

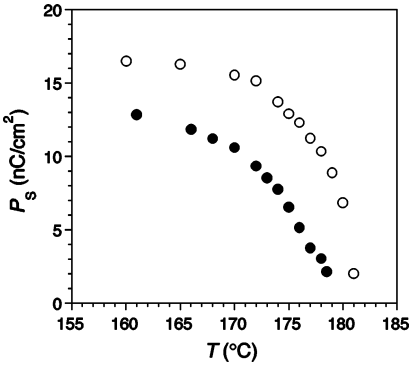

Figure 6. Absolute value of spontaneous polarization (P_S) as a function of temperature (T) for (*R*)-**3** before (filled circles) and after deuterium exchange (open circles) in 1:1 $CD_3OD/CDCl_3$.

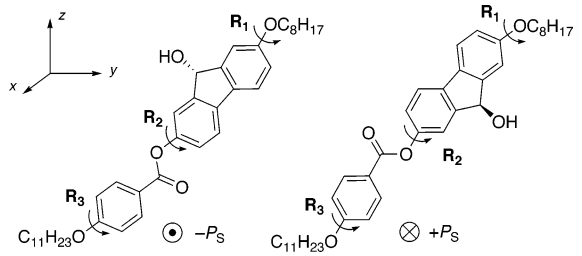

Figure 7. Two orientations of (*R*)-**3** with the plane of the fluorenone core congruent to the tilt plane of the SmC* phase (*y*,*z*). The corresponding P_S vectors point from negative to positive along the polar *x*-axis according to the physics convention.[11]

chains are fully extended in anti conformations (Figure 7). Given these constraints, there are three rotational degrees of freedom (R_1-R_3) controlling the shape of the mesogen (*R*)-**3**. In the minimized AM1 structures, the two alkoxy groups are coplanar with the fluorenol (R_1) and benzoate units (R_3), either syn or anti relative to the carbinol and carbonyl groups, respectively. The carboxyl group is out-of-plane with respect to the fluorenol unit with a dihedral angle of ca. 50° (R_2). There are two degenerate conformations in which the carbonyl group is syn oriented relative to the carbinol group and two degenerate conformations in which the carbonyl group is anti oriented. The carboxyl group has therefore no net dipole moment along the polar axis when the plane of the fluorenol core is congruent with the tilt plane. Based on this analysis, eight different conformations were obtained for each P_S orientation by permutations of R_1, R_2, and R_3 (see Supporting Information).

The calculated heats of formation of the sixteen conformations are approximately equal, ranging from −220.01 to −220.45 kcal/mol, but the conformations vary significantly in terms of their shape, from rodlike to bow-like. To identify the most likely contributors to the conformational distribution of (*R*)-**3** in the lamellar SmC* phase, each conformation was rigidly tilted in the *y*,*z*-plane to give an end-to-end distance along the *z*-axis (layer normal) equal to the layer spacing of 31.8 Å measured by powder X-ray diffraction. The optical tilt angle θ_{opt} of each conformation, as defined by the angle formed by the long axis of the core (assumed to be the axis linking C-7 and C-4′) and the layer normal, was calculated from the Cartesian coordinates of the model using the

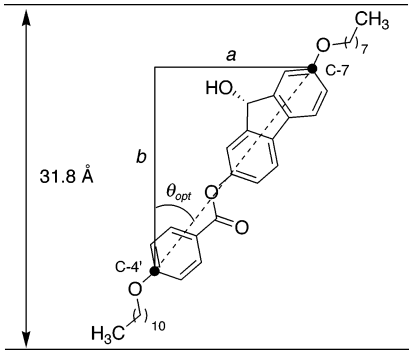

Figure 8. Calculation of the optical tilt angle θ_{opt} for a molecular model of (*R*)-**3** tilted in the *y*,*z*-plane as $\theta_{opt} = \tan^{-1}(a/b)$.

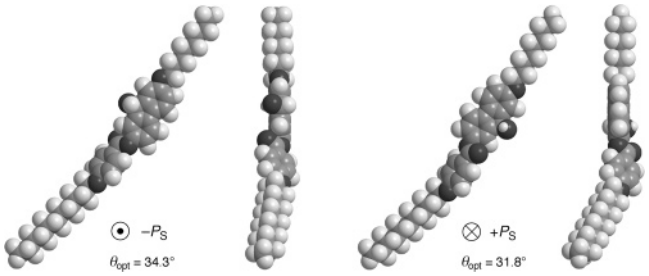

Figure 9. Molecular models of (*R*)-3 with positive and negative P_S orientations with θ_{opt} values closest to the experimental value of 32°, as side-on (left) and end-on views (right).

formula $\theta_{opt} = \tan^{-1}(a/b)$ (Figure 8).[23] The resulting θ_{opt} values range from 23.5° to 53.6° for the $-P_S$ conformations, and from 19.4° to 46.5° for the $+P_S$ conformations. Remarkably, the $+P_S$ and $-P_S$ conformations with θ_{opt} values closest to the experimental value of 32° are very similar from a side-on view, but the $+P_S$ conformation reveals a significant bend of the alkoxy side-chain out of the tilt plane, which may be less favored in the lamellar structure of the SmC* phase (Figure 9). This difference, albeit very subtle, may account for the negative spontaneous polarization of (*R*)-**3**, intermolecular interactions notwithstanding.

Discussion

The experimental results presented herein, including phase transition temperatures and FT-IR experiments, strongly suggest that intermolecular hydrogen bonding stabilizes the SmC* phase formed by (*R*)-**3**. However, the results of the dilution experiments are inconsistent with the formation of an extended polar hydrogen bond network, as initially envisioned, and suggest instead that polar order is enhanced by the formation of antiparallel dimers via OH−O═C hydrogen bonding interactions (Figure 10). The different effects observed in the dilution experiments may be explained by the propensity of the additives to (a) disrupt dimer formation (negative deviation), (b) dilute undisturbed dimers (no deviation), or (c) promote the aggregation of dimers to give more highly ordered polar aggregates (positive devia-

(23) In conventional SmC* liquid crystals, the optical tilt angle is that described by the long axis of the aromatic core, which is more birefringent than the side-chains due to its higher polarizability, and the smectic layer normal. Bartolino, R.; Doucet, J.; Durand, G. *Ann. Phys.* **1978**, *3*, 389.

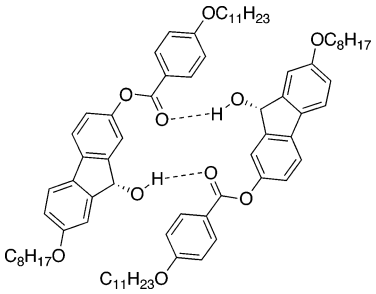

Figure 10. Proposed antiparallel fluorenol dimer structure.

tion). In the two cases of additives causing a nonlinear decrease in P_o (**11** and **PPz**), it is interesting to note that P_o falls below the detection limit when the ratio of fluorenol to additive is approximately 1:1, which is consistent with a complete disruption of fluorenol dimers. The nonlinear changes in P_o upon dilution of (*R*)-**3** with **11**, **2-PPy** and **PPz** may be related to the propensity of the additive cores to form strong π-stacking interactions with the fluorenol (**11**, **2-PPy**),[24] or to act as a strong hydrogen bond acceptor that may disrupt the OH−O═C bonds of the fluorenol dimer (**PPz**). However, it is still unclear why the planar **11** would disrupt dimer formation whereas the planar **2-PPy** would promote their aggregation. Perhaps this is due to the unique ability of **2-PPy** to π-stack *and* act as a good hydrogen bond acceptor. The two additives that produced a linear decrease in P_o have nonplanar cores that cannot π-stack as effectively with the planar fluorenol, with lesser (**5-PPy**) or no hydrogen bond accepting ability (**BPh**) relative to **PPz**.

Further evidence supporting the hydrogen-bonded dimer model is provided by the deuterium exchange experiment, which, at first glance, appears to be inconsistent with our assumption that intermolecular hydrogen bonding enhances polar order. Indeed, the perturbation of intermolecular hydrogen bonds between neutral molecules by substitution of a deuteron for a proton normally results in weaker interactions.[25] In classical H/D fractionation experiments in which proteins are dissolved in protic solvents of varying H/D composition, the deuterium content of functional groups forming hydrogen bonds is inversely proportional to the hydrogen bond strength; i.e., hydrogen bonding discriminates against the heavier isotope.[22] In this case, we must consider the spectroscopic evidence, which is consistent with an equilibrium between two hydrogen bonding interactions of different strengths, OH−OH and OH−O═C, in the SmC* phase formed by (*R*)-**3**. Hence, it is possible that deuterium exchange causes a shift in the hydrogen bond equilibrium favoring the weaker OH−O═C interactions over the stronger OH−OH interactions,[26] which would explain the increase in P_S if one assumes that OH−O═C interactions are primarily responsible for the increase in polar order via the formation of antiparallel dimers.

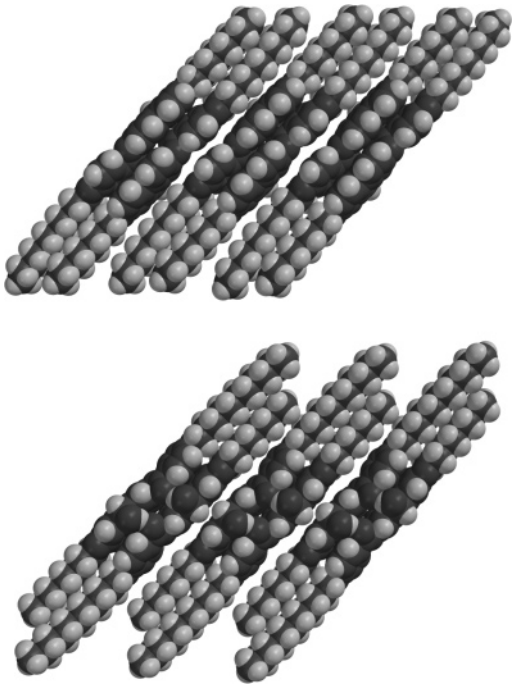

Figure 11. Molecular models of (*R*)-3 as hydrogen-bonded antiparallel dimers with negative P_S (top) and positive P_S (bottom) orientations along the polar axis, which is perpendicular to the page.

Modeling of the antiparallel dimer using the MMFF force field predicts that (*R*)-**3** dimerizes in a π-facial geometry (Figure 11), which imparts a rotational bias about the director **n** favoring a negative polarization that is less subtle than for the monomeric form. In this geometry, the dimer transverse dipole moment is oriented approximately parallel to the fluorenol planes and perpendicular to the molecular long axis. As shown in Figure 11, rotation of the dimer about **n** in a tilted smectic layer frame gives two rotational states with opposite signs of P_S, and with very different packing properties. The rotational state with negative P_S can pack into a smectic layer without creating any excluded volume, whereas the rotational state with positive P_S would create a significant amount of excluded volume in a multilayer arrangement. Such a difference in packing properties would raise the energy of the positive P_S rotational state in the condensed SmC* phase relative to the negative P_S state.

Conclusions

We have shown that the mesogen (*R*)-**3**, which features a fluorenol core as its only element of chirality, forms a ferroelectric SmC* phase that appears to be stabilized by intermolecular hydrogen bonding, with a measurable spontaneous polarization of −10.7 nC/cm^2 at $T - T_C = -10$ K. Molecular modeling based on the Boulder model suggests that the intrinsic conformational bias favoring one orientation of the fluorenol dipole moment along the polar axis of the SmC* phase is very subtle and implies that self-assembly via hydrogen bonding may play a role in enhancing polar order. Results from FT-IR spectroscopy, dilution with achiral SmC additives, and deuterium exchange experiments suggest that polar order is enhanced by the formation of

(24) Ab initio calculations suggest that 2-phenylpyrimidine adopts a planar conformation in the ground state, whereas 5-phenylpyrimidine adopts a twisted conformation with a dihedral angle of 43.1° between the two rings. Barone, V.; Commisso, L.; Lelj, F.; Russo, N. *Tetrahedron* **1985**, *41*, 1915.

(25) Hibbert, F.; Emsley, J. In *Advances in Physical Organic Chemistry*; Bethell, D., Ed.; Academic Press: London, 1990; Vol. 26, p 255−379.

(26) Moskala, E. J.; Howe, S. E.; Painter, P. C.; Coleman, M. M. *Macromolecules* **1984**, *17*, 1671.

fluorenol dimers via relatively weak OH−O═C interactions. Such self-assembly should increase the rotational order about the long molecular axis and, therefore, the orientational bias of the fluorenol transverse dipole moment along the polar axis that gives rise to P_S. The role played by hydrogen bonding self-assembly in enhancing polar order in a ferroelectric liquid crystal is unprecedented, and it raises the possibility of designing new generations of SmC* mesogens with functionalities capable of forming stronger hydrogen bond interactions such as OH−N, for example. We have therefore undertaken the synthesis and characterization of a series of chiral azafluorenol mesogens using a similar directed metalation cross-coupling route, which will be reported in due course.

Acknowledgment. We are grateful to the Natural Sciences and Engineering Research Council of Canada, the Canada Foundation for Innovation and the Ontario Challenge Fund for support of this work. We also thank Patricia Basque of the CERSIM at Université Laval for performing the powder X-ray measurements.

Supporting Information Available: Full experimental details including synthetic procedures, full characterization of new compounds, physical measurement procedures, and molecular models in PDF format. This material is available free of charge via the Internet at http:// pubs.acs.org.

CM047860P